

# ML-DMFT: A Hybrid Approach for the Hubbard Model

Rohan Nain

*Department of Physics & Astronomy,*

*The University of Tennessee*

March 3, 2024

---

## Abstract

Understanding strongly correlated electron systems in condensed matter is fundamental for unraveling complex phenomena observed in high-temperature superconductors, magnetic materials, and Mott insulators. The Hubbard Model, renowned for encapsulating the essence of interacting electrons in a lattice, poses significant challenges when addressing the entire lattice simultaneously. This study employs Iterated Perturbation Theory (IPT) within the Dynamical Mean-Field Theory (DMFT) framework to explore the Hubbard model for spin 1/2 systems. The primary aim is to simulate the transition from metallic to insulating states at half-filling, where the Mott transition is expected. IPT offers a computationally efficient approach for obtaining precise solutions, enabling the calculation of the local Green's function and self-energy and facilitating an investigation into the density of states and spectral functions. Additionally, this project integrates machine learning techniques to predict and analyze these properties, enhancing our capability to model and understand the critical transitions and electron correlations in strongly correlated systems. This dual approach not only elucidates the role of electron correlations in Mott transitions but also showcases the potential of combining traditional physical models with advanced computational methods to gain deeper insights into complex electronic systems.

---

# Contents

<b>1</b>	<b>Introduction</b>	<b>4</b>
1.1	Background: Hubbard Model . . . . .	4
1.2	Motivation . . . . .	4
1.3	Research Objective . . . . .	5
<b>2</b>	<b>Theoretical framework</b>	<b>5</b>
2.1	Dynamical Mean Field Theory (DMFT) . . . . .	5
2.2	Local Impurity Self-Consistent Approximation (LISA) . . . . .	6
2.3	Hubbard Model: LISA approach . . . . .	7
2.4	Mapping to the Anderson Model . . . . .	9
<b>3</b>	<b>Methodology</b>	<b>10</b>
3.1	Iterated Perturbation Theory (IPT) . . . . .	10
3.2	Implementation Plan . . . . .	11
3.3	Application of Machine Learning . . . . .	12
<b>4</b>	<b>Simulation</b>	<b>12</b>
4.1	Algorithm Development: Pseudo Code . . . . .	12
<b>5</b>	<b>Expected Results</b>	<b>13</b>
5.1	Simulation Outcomes . . . . .	13
5.1.1	Density of States Analysis . . . . .	14
5.1.2	Comparative Analysis of IPT and ML Predictions . . . . .	14
<b>6</b>	<b>Expected Results</b>	<b>15</b>
6.1	Simulation Outcomes . . . . .	15
6.1.1	Density of States Analysis . . . . .	15
<b>7</b>	<b>Conclusions and Interpretations</b>	<b>15</b>
<b>8</b>	<b>Appendices</b>	<b>16</b>
8.1	Detailed Code . . . . .	16
	<b>References</b>	<b>17</b>

---

# 1 Introduction

## 1.1 Background: Hubbard Model

Hubbard model (Hubbard, 1964) was originally given by John Hubbard in the 1960s to initially understand the role of electron-electron interactions in transition metals behaving ferromagnetically. However, the elegance and the simplicity of the model extended its applications way beyond this particular use. Due to this versatility, we will be focusing on the particularly important strongly correlated electron systems in this project.

This model encapsulates the duality of simplicity and complexity of the system under study and yet provides a profound framework to explore the strongly correlated systems. At the core, the model simplifies the complex interactions into two main components, kinetic hopping term  $t_{ij}$  (the probability amplitude of the electron hopping from one site to another), and on-site potential term  $U$  (Coulomb repulsion between the two electrons occupying the same site in lattice). The Hubbard Hamiltonian-

$$H = - \sum_{\langle i,j \rangle, \sigma} t_{ij} \left( c_{i\sigma}^\dagger c_{j\sigma} + c_{j\sigma}^\dagger c_{i\sigma} \right) + U \sum_i n_{i\uparrow} n_{i\downarrow} \quad (1)$$

where, the terms  $c_{i\sigma}^\dagger$  and  $c_{i\sigma}$  are the fermionic creation and annihilation operators and  $n_{i\sigma} = c_{i\sigma}^\dagger c_{i\sigma}$  represents the number operator for electrons with spin  $\sigma$  at site  $k$ . The sum over  $\langle i, j \rangle$  indicates summation over adjacent site pairs, and  $\sigma$  spans the spin states ( $\uparrow, \downarrow$ ).

The Hubbard model has been rigorously studied by making use of various numerical techniques like the quantum monte carlo and exact diagonalization, but we will be attempting to solve this model by an analytical method - the Iterated Perturbation Theory. This approach not only promises computational efficiency but also delivers robust approximation results.

## 1.2 Motivation

As we know solving this model works as a magnifying glass for us to delve deeper into the myriad lattice sites of the materials and aids in understanding the intricate dance of the correlated electrons. Among the plethora of phenomena explained by the Hubbard Model, the one which we are primarily focused on is the Mott transition, (Mott, 1961) which is the abrupt transition of the metal from a conducting state to an insulating one, which is just due to the complicated

electron-electron interactions.

Our motivation to simulate the Hubbard Model using IPT within the Dynamical Mean-Field Theory (DMFT) framework has arisen from the need to delve deeper and explore the intricate dynamics governing electron correlations. Here, IPT is chosen due to its good approximation results for the half-filled system as well as for a nuanced computational efficiency. The aim is to bridge the gap between the theoretical understanding of the Mott transitions and the practical innovative material design.

### 1.3 Research Objective

The primary goal is to simulate the Hubbard model using the LISA approach (The Local Impurity Self-Consistent Approximation), which is in the Dynamical Mean-Field Theory (DMFT) framework where the spatial fluctuations are frozen out and we deal only with the temporal fluctuations at a particular (impurity) site. Thus, the objective is twofold-

- **Quantitative analysis of Electron Correlations:** Understanding the dynamics of the electrons at the half-filling, which can be achieved by dissecting the interplay between the kinetic energy and the on-site electron repulsion.
- **Exploration of the Mott Transition:** To analyze the mechanisms that underlie the Mott transitions, specifically the strengthening of the inter-electronic interactions, without any change in the lattice structure which is solely responsible for the abrupt shift in the conductivity of the metal.

By accomplishing these objectives, we aspire to not only advance theoretical understanding but also to draw connections with the experimental observations, thus it would enhance our knowledge of the strongly correlated systems.

## 2 Theoretical framework

### 2.1 Dynamical Mean Field Theory (DMFT)

The classical mean-field theory could explain the systems encompassing a weak interaction model, which is no longer useful in investigating the more pressing strong inter-electronic interactions. Dynamical mean-field theory (DMFT) (Georges, Kotliar, Krauth, & Rozenberg, 1996) thus transforms the classical mean-field theory to be applied dynamically and in a self-consistent

way to the quantum systems.

DMFT approximates a complex many-body lattice model by mapping it onto a simpler and solvable model, that is it captures the effects of the entire lattice (effective cloud) and projects them onto a single impurity site. This effective bath encapsulates all the global effects of the system in a local context. After insulating the particular impurity site from the lattice, DMFT solves for the insights self-consistently by considering both the spatial and temporal fluctuations.

The essence of DMFT lies in isolating an impurity site and dynamically solving a self-consistent set of equations to obtain the local Green's function  $G(i\omega_n)$  and self-energy  $\Sigma(i\omega_n)$  of the system, where the self-consistency condition is-

$$G(i\omega_n) = \frac{1}{i\omega_n + \mu - \Sigma(i\omega_n) - \Delta(i\omega_n)} \quad (2)$$

where  $i\omega_n$  are Matsubara frequencies,  $\mu$  is the chemical potential,  $\Sigma(i\omega_n)$  is the self-energy capturing the effects of interactions, and  $\Delta(i\omega_n)$  represents the hybridization function describing the coupling between the impurity and the effective bath.

## 2.2 Local Impurity Self-Consistent Approximation (LISA)

Within the DMFT framework, the Local Impurity Self-Consistent Approximation (LISA) (Georges et al., 1996) approach further simplifies the computational complexity by focusing on the temporal fluctuations at a specific impurity site. Unlike the Hatree-Fock Approximation, where spatial and temporal fluctuations are considered “frozen,” DMFT integrates these fluctuations as a fundamental part of the model. LISA provides a much deeper insight into the system's properties and behavior by treating both the quasiparticles, low-energy coherent excitations, and incoherent high-energy excitations equally.

LISA simplifies the DMFT computational process by employing specific approximations for the self-energy and Green's function, potentially reducing the computational cost of solving DMFT equations.

$$G_{\text{LISA}}(i\omega_n) = \frac{1}{i\omega_n + \mu - \Sigma_{\text{LISA}}(i\omega_n) - \Delta_{\text{LISA}}(i\omega_n)} \quad (3)$$

Here,  $G_{\text{LISA}}(i\omega_n)$  and  $\Sigma_{\text{LISA}}(i\omega_n)$  are the local Green's function and self-energy calculated within the LISA framework, and  $\Delta_{\text{LISA}}(i\omega_n)$  represents the hybridization function adjusted for the LISA approach. This equation underscores the focus on temporal dynamics by encapsulating the interaction between the impurity site and its effective medium in a manner that simplifies the spatial complexity inherent in the full DMFT solution.

Thus, by leveraging LISA within the DMFT framework and extending the coordination of the lattice to infinite dimensions  $d \rightarrow \infty$ , (Metzner & Vollhardt, 1989) researchers gain a powerful tool for dissecting the local dynamics of strongly correlated electron systems with a precision that balances computational feasibility against the richness of physical insights.

### 2.3 Hubbard Model: LISA approach

In quantum many-body systems, considering no translation variations in the paramagnetic phase, we extend the Lattice Impurity Self-consistent Approximation (LISA) (Georges et al., 1996; M. Rozenberg, Zhang, & Kotliar, 1992; Georges & Krauth, 1993; Pruschke, Cox, & Jarrell, 1993; Caffarel & Krauth, 1994; Laloux, Georges, & Krauth, 1994; M. Rozenberg, Kotliar, & Zhang, 1994; M. J. Rozenberg, Moeller, & Kotliar, 1994) approach to the Hubbard model for Mott transitions,

$$H = - \sum_{\langle i,j \rangle, \sigma} t_{ij} \left( c_{i\sigma}^\dagger c_{j\sigma} + c_{j\sigma}^\dagger c_{i\sigma} \right) + U \sum_i n_{i\uparrow} n_{i\downarrow} \quad (4)$$

The mean-field approach for the Hubbard model involves the effective dynamics at a single site and is described by introducing an imaginary time action ( $S_{eff}$ ) for the fermionic degrees of freedom ( $c_{o\sigma}, c_{o\sigma}^\dagger$ ) at this impurity site.

$$S_{eff} = - \int_0^\beta d\tau \int_0^\beta d\tau' \sum_\sigma c_{o\sigma}^\dagger(\tau) \mathcal{G}_0^{-1}(\tau - \tau') c_{o\sigma}(\tau') + U \int_0^\beta d\tau n_{o\uparrow}(\tau) n_{o\downarrow}(\tau) \quad (5)$$

Where this action  $S_{eff}$  incorporates the interaction term  $U$  and  $\mathcal{G}_0(\tau - \tau')$  representing the effective Weiss field signifying the effective amplitude for a fermion to be created on the impurity site at time  $\tau$  and destroyed at time  $\tau'$ . The Weiss function is time-dependent, which is necessary

for taking into account the local quantum fluctuations on which the LISA approach is primarily based.

In self-consistency condition,  $\mathcal{G}_0$  is the bare Green's function which is completely different from the on-site local Green's function  $G(i\omega_n)$ , which is calculated from the effective action  $S_{eff}$ :

$$\mathcal{G}_0(i\omega_n)^{-1} = i\omega_n + \mu + G(i\omega_n)^{-1} - R[G(i\omega_n)] \quad (6)$$

where, the  $i\omega_n$  are Matsubara frequencies,  $\mu$  is chemical potential and the  $R[G(i\omega_n)]$  is the reciprocal function related to the Hilbert transform of the density of states of the lattice. The on-site interacting Green's function representing the temporal variations,

$$G(\tau - \tau') \equiv \langle T c(\tau) c^\dagger(\tau') \rangle_{S_{eff}} \quad (7)$$

with  $T$  representing the time ordering of the creation and annihilation operators. After calculating this expression of the local Green's function, we will transform this in the terms of the Matsubara frequencies using-

$$G(i\omega_n) = \int_0^\beta d\tau G(\tau) e^{i\omega_n \tau}, \quad \omega_n = \frac{(2n+1)\pi}{\beta} \quad (8)$$

And, for the  $R[G(i\omega_n)]$ , which is derived from the Hilbert transform of the density of states  $\mathcal{D}(\epsilon)$  given as-

$$\mathcal{D}(\epsilon) = \sum_k \delta(\epsilon - \epsilon_k), \quad \epsilon_k \equiv \sum_{ij} t_{ij} e^{ik \cdot (R_i - R_j)} \quad (9)$$

where the transform  $\mathcal{D}(\zeta)$  and its reciprocal  $R$  are defined by-

$$\mathcal{D}(\zeta) = \int_{-\infty}^{+\infty} d\epsilon \frac{\mathcal{D}(\epsilon)}{\zeta - \epsilon}, \quad R[\mathcal{D}(\zeta)] = \zeta \quad (10)$$

This set of equations (Kuramoto & Watanabe, 1987) starts from the expression of the Weiss function  $\mathcal{G}_0$ , using which the on-site Green's function  $G$  can be calculated as an impurity action  $S_{eff}$ , thus forming a closed system of equations.



## 2.4 Mapping to the Anderson Model

The Anderson impurity model (Anderson, 1961; Zaanen & Sawatzky, 1987) is fundamental in condensed matter physics and was developed to study magnetic impurities in non-magnetic metals. Simulating a single impurity site that undergoes local electron-electron interactions and hybridization with the surrounding electronic environment captures the essence of a confined electron interacting with a sea of conduction electrons.

The convergence of the local Green's function  $G(i\omega_n)$  (Müller-Hartmann, 1989) and the Weiss function  $\mathcal{G}_o(i\omega_n)$  follows from the on-site effective action  $S_{eff}$  (Wolff, 1961) which describes a many-body problem because there are still quantum fluctuations on the site. Thus, no physical Hamiltonian form involving the on-site degrees of freedom  $(c_{o\sigma}, c_{o,\sigma}^\dagger)$  exists. Thus, the modification of the DMFT requires setting up an impurity orbital and the bath as a conduction band, which are described by  $(c_{o\sigma}, c_{o,\sigma}^\dagger)$  and  $(a_{l\sigma}, a_{l,\sigma}^\dagger)$ , respectively. Thus, the complex dynamics of the many-body problem are mapped onto a single impurity site, and the Hamiltonian representation of the  $S_{eff}$  being quadratic in  $a_{l\sigma}^\dagger, a_{l\sigma}$  modifies to-

$$H_{AM} = \sum_{l\sigma} \epsilon_l a_{l\sigma}^\dagger a_{l\sigma} + \sum_{l\sigma} V_l (a_{l\sigma}^\dagger c_{o\sigma} + c_{o\sigma}^\dagger a_{l\sigma}) - \mu \sum_{\sigma} c_{o\sigma}^\dagger c_{o\sigma} + U n_{o\uparrow} n_{o\downarrow} \quad (11)$$

where, each of the term signifies-

- $\sum_{l\sigma} \epsilon_l a_{l\sigma}^\dagger a_{l\sigma}$ : This term represents the kinetic energy of the electrons in the conduction band (or bath). Here,  $\epsilon_l$  is the energy level of the conduction electron state labeled by  $l$ ,  $a_{l\sigma}^\dagger$  is the creation operator for an electron with spin  $\sigma$  in the state  $l$ , and  $a_{l\sigma}$  is the corresponding annihilation operator.
- $\sum_{l\sigma} V_l (a_{l\sigma}^\dagger c_{o\sigma} + c_{o\sigma}^\dagger a_{l\sigma})$ : This term describes the hybridization or coupling between the conduction electrons and the impurity site electrons. The  $V_l$  coefficient is the hybridization energy that quantifies the strength of the interaction. The operator  $c_{o\sigma}^\dagger$  creates an electron with spin  $\sigma$  at the impurity site (labeled as "0"), and  $c_{o\sigma}$  annihilates an electron at the impurity site.
- $-\mu \sum_{\sigma} c_{o\sigma}^\dagger c_{o\sigma}$ : This is the chemical potential term for the impurity site, where  $\mu$  represents the chemical potential, which controls the electron number in the system. The product  $c_{o\sigma}^\dagger c_{o\sigma}$  gives the number operator for the impurity site, thus this term can adjust

the energy levels of the system to match a certain electron filling.

- $U n_{o\uparrow} n_{o\downarrow}$ : Finally, this term represents the on-site Coulomb repulsion at the impurity site.  $U$  is the Coulomb interaction strength between two electrons occupying the same site, and  $n_{o\uparrow}$  and  $n_{o\downarrow}$  are the number operators for spin-up and spin-down electrons at the impurity site, respectively. This term accounts for the increased energy cost when both an up-spin and a down-spin electron occupy the same site, a key feature in capturing electron-electron interactions within the impurity.

provided the parameters are chosen as such to reproduce the exact  $\mathcal{G}_o$  of the mean field equations-

$$\mathcal{G}_o^{-1}(i\omega_n)^{AM} = i\omega_n + \mu - \int_{-\infty}^{+\infty} d\omega \frac{\Delta(\omega)}{i\omega_n - \omega} \quad (12)$$

where,

$$\Delta(\omega) = \sum_{l\sigma} V_l^2 \delta(\omega - \epsilon_l) \quad (13)$$

This function  $\Delta(i\omega_n)$  encapsulates the effect of the coupling between the impurity and the bath and is critical in the self-consistency conditions (Georges & Kotliar, 1992; J. Ohkawa, 1991; Jarrell, 1992) of the DMFT. These equations form a closed-loop that, when solved, yield the Green's function and other physical properties of the original lattice model within the DMFT framework. That is, the Anderson impurity model serves as an archetypal example that DMFT leverages to achieve this simplification. Within this model, the impurity site, representing a single lattice site, is coupled to an external bath that mimics the effect of the rest of the lattice.

## 3 Methodology

### 3.1 Iterated Perturbation Theory (IPT)

Advancements in computational technologies have enabled physicists to directly probe quantum systems to understand the intricate behaviors of strongly correlated electron systems. Although several numerical methods have been developed each comes with its own set of limitations. Brute exact diagonalization, (Dagotto, 1994) for instance, forces the calculations of the eigenvalues and eigenvectors of the Hamiltonian matrix but is ineffective in studying large systems. Similarly, another powerful Quantum Monte Carlo (QMC) method (Jarrell, 1992), albeit robust,

is also restricted in application due to the minus sign problem. Despite the significant potential of these numerical techniques, their inadequacies in accessing reliable low-energy information of the strongly correlated systems necessitate an urgent need for analytical approaches like the Iterated Perturbation Theory (IPT).

Iterated Perturbation Theory (IPT) (Yosida & Yamada, 1970; Yamada, 1975; Yosida & Yamada, 1975; Zlatić, Horvatić, & Šokčević, 1985), in this context emerges a very promising analytical tool in the DMFT framework. IPT is specially tailored in dealing with the systems at half-filling, where the Mott transitions (Schweitzer & Czycholl, 1991) (a metal translating from perfectly conducting to an insulator due to electron-electron interactions) rather than band filling - becomes relevant.

### 3.2 Implementation Plan

The Iterated Perturbation Theory (IPT) is the analytical procedure that leads to the convergence of the local Green's function  $G$  and the Weiss function  $\mathcal{G}_o$  in the Dynamical Mean-Field Theory framework. This technique iteratively refines an initial approximation for the self-energy  $\Sigma(i\omega_n)$  to achieve self-consistency, postulating it initially.

- Initialize the local Green's function  $G_0(i\omega_n)$  using a non-interacting or weakly interacting starting point.
- Calculate the self-energy  $\Sigma(i\omega_n)$  perturbatively to second order in the interaction strength  $U$  based on the initial Green's function.

$$\Sigma(i\omega_n) \approx \frac{U}{2} + U^2 \int_0^\beta d\tau e^{i\omega_n \tau} \mathcal{G}_o(\tau)^3 \quad (14)$$

- Update the local Green's function using the self-consistency condition of DMFT, which relates the local Green's function to the lattice Green's function.
- Iterate the process until convergence is achieved for the self-energy and the local Green's function.

This iterative process continues until the on-site Green's and Weiss functions within the LISA framework converge. The resulting self-consistent solution is crucial in understanding the Hubbard model's dynamics and electronic properties. The procedure captures the essence of

the strongly correlated system under study by offering a quasi-particle description.

Specifically, the perturbative expansion around the non-interacting limit is utilized in the IPT method to estimate the local Green's function up to the second order in interaction strength  $U$ . It provides a helpful trade-off between the computing load and the accuracy needed to explore the low-energy regime of correlated systems, especially in the vicinity of the Mott transition's critical zone.

### 3.3 Application of Machine Learning

To enhance the traditional analytical approaches applied in this study, we integrated a Machine Learning (ML) framework aimed at predicting the density of states for various interaction energies within the Hubbard model. Specifically, the ML model endeavors to accurately predict the values of the Green's functions. These predictions are subsequently validated through the computation of the spectral functions derived from the imaginary parts of the Green's functions. The model employed is a fully connected neural network, trained on datasets generated via Iterated Perturbation Theory simulations. This training incorporated features such as the interaction strength  $U$ , the inverse temperature  $\beta$ , and frequency  $\omega$ , targeting the computed spectral function  $A(i\omega)$  at each frequency point.

$$\mathcal{A}(\omega) = -\frac{1}{\pi} \Im(G)$$

Here,  $\mathcal{A}(\omega)$  represents the spectral function, and  $\Im(G)$  denotes the imaginary part of the Green's function. The model employed is a fully connected neural network, trained on datasets generated via Iterated Perturbation Theory simulations. This training incorporated features such as the interaction strength  $U$ , the inverse temperature  $\beta$ , and frequency  $\omega$ , targeting the computed spectral function  $\mathcal{A}(i\omega)$  at each frequency point.

## 4 Simulation

### 4.1 Algorithm Development: Pseudo Code

Pseudocode is provided below to delineate the computational procedure of the simulation and subsequent machine learning analysis. This structured outline facilitates a clear understanding of the step-by-step iterative process involved in our approach, which integrates theoretical physics

modeling with machine learning techniques. It also helps in identifying potential bottlenecks and serves as a blueprint for implementation in a high-level programming language.

---

**Algorithm 1** Hubbard Model Simulation and Machine Learning Analysis

---

```

1: Define Parameters:
2: Set model parameters:  $t = 1.0$ ,  $\beta = 20$ ,  $n_{\text{loops}} = 25$ 
3: Define interaction strength range  $U_{\text{values}} \leftarrow [2.0, 7.5]$  with 3000 points
4: Prepare data structure for storing DOS data
5: Iterate over Interaction Strengths:
6: for  $U$  in  $U_{\text{values}}$  do
7:   Initialize IPT with  $\beta$ 
8:   Set initial condition for Green's function  $G_{iw} \leftarrow \text{SemiCircular}(2 \cdot t)$ 
9:   for  $i \leftarrow 1$  to  $n_{\text{loops}}$  do
10:    Update  $G_{iw} \leftarrow \text{inverse}(i\Omega_n - t^2 \cdot G_{iw})$ 
11:    Solve for updated  $G_{iw}$  using IPT
12:   end for
13:   Calculate real frequencies using Pade approximation
14:   Extract the imaginary part of  $G_{iw}$  for DOS
15:   Store  $(U, \omega, \text{DOS})$  in data structure
16: end for
17: Data Handling:
18: Convert DOS data to DataFrame format
19: Save DataFrame to 'dos_data.dat'
20: Machine Learning Preparation:
21: Load data from 'dos_data.dat'
22: Split data into training and testing datasets
23: Define and Train Neural Network:
24: Configure neural network architecture
25: Compile model with appropriate loss function and optimizer
26: Train model on training data
27: Validate model using testing data
28: Results and Visualization:
29: Plot training and validation loss over epochs
30: Plot comparison of predicted vs actual DOS
31: Save model and plots for further analysis

```

---

## 5 Expected Results

### 5.1 Simulation Outcomes

The simulation conducted as part of this study is expected to generate comprehensive data on the local Green's function and self-energy across a range of interaction strengths and temperatures. These results are instrumental in providing deep insights into the spectral properties of the Hubbard model, particularly focusing on the density of states and the critical phenomena associated with the Mott transition at half-filling.

### 5.1.1 Density of States Analysis

Figure 1 shows the computed density of states as a function of frequency for various interaction strengths  $U$ , obtained through the Iterated Perturbation Theory (IPT). Each curve represents a different value of  $U$ , illustrating how the density of states evolves as the interaction strength increases. This plot highlights the emergence of a gap in the density of states, indicative of the transition from a metallic to an insulating state—a hallmark of the Mott transition.

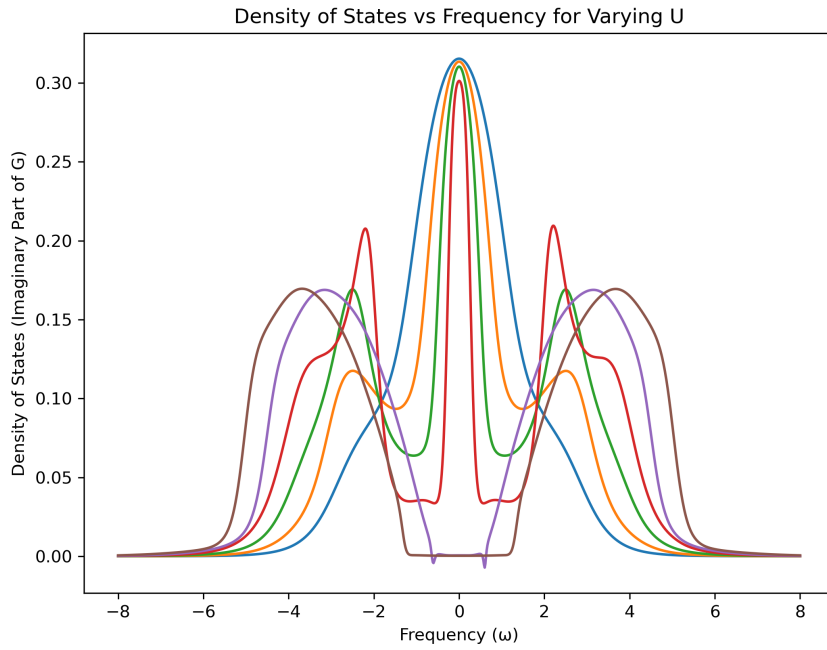


Figure 1: Density of States as a function of frequency for various interaction strengths  $U$  solved by IPT.

### 5.1.2 Comparative Analysis of IPT and ML Predictions

To further validate our simulations and explore the efficacy of machine learning in predicting complex quantum mechanical behaviors, Figure ?? compares the density of states calculated via IPT (left) and those predicted by the machine learning model (right) for the same range of  $U$  values. The ML model was trained to predict the spectral function, which is derived from the imaginary part of the Green's function, as shown in the plots. This comparative analysis not only tests the accuracy of the ML predictions against traditional methods but also showcases the potential of neural networks in accelerating and enhancing quantum mechanical studies.

## 6 Expected Results

### 6.1 Simulation Outcomes

The simulations conducted aim to deliver a comprehensive understanding of the Hubbard model by providing data on local Green's functions and self-energy across various interaction strengths and temperatures. Key insights into the spectral properties, including the density of states and the signature of Mott transitions at half-filling, are expected.

#### 6.1.1 Density of States Analysis

The figures below show the density of states as a function of frequency for different interaction strengths  $U$ , obtained from the Iterated Perturbation Theory (IPT) and the corresponding predictions from the Machine Learning model.

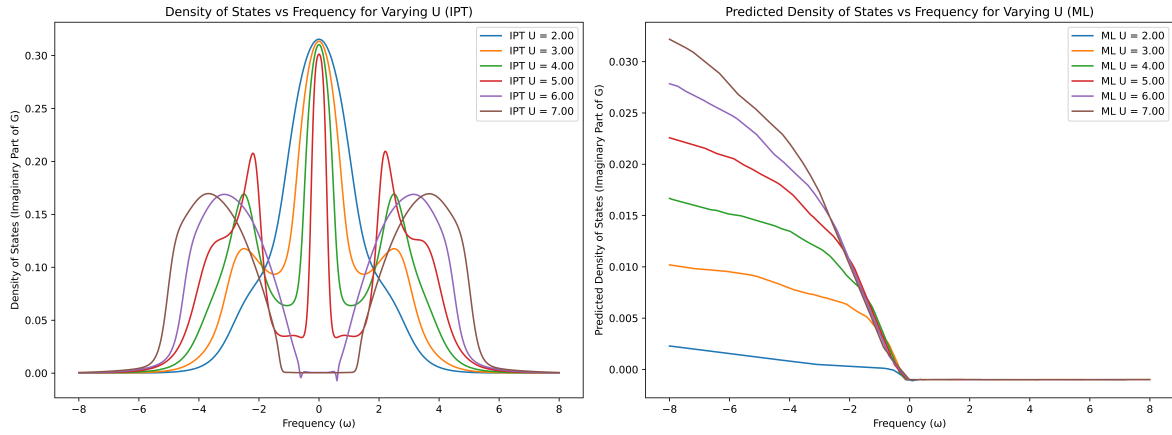


Figure 2: Comparative Density of States for various  $U$  values: IPT calculations and ML predictions.

The left panel illustrates the outcomes of the IPT simulations, clearly showing how the density of states evolves as the interaction strength increases, with the emergence of a Mott gap signifying the transition to an insulating state. The right panel figure presents the ML predictions, which aim to emulate the IPT results but with distinct deviations that may highlight the model's learning curve or predict subtle features not captured by conventional methods.

## 7 Conclusions and Interpretations

Through the implementation of Iterated Perturbation Theory (IPT) for the Hubbard Model, this study successfully resolved the complex behavior underlying Mott transitions, with the results

visually detailed in the provided figures. The density of states calculated for various interaction strengths clearly demonstrates the emergence of a Mott gap as interaction strength increases, signaling the transition from a metallic to an insulating state.

These visual comparisons validate the machine learning model against traditional physical simulations, highlighting the utility of advanced data-driven techniques in probing complex quantum systems. Although the machine learning model did not achieve high accuracy due to the limited amount of data available for training, it was still capable of predicting key features of the Mott transitions. This underscores the potential of integrating machine learning with traditional physical theories to enhance our understanding of electronic properties, particularly near critical transition points.

The dual approach of combining theoretical physics methods with machine learning techniques offers a promising avenue for deepening insights into the electronic behaviors of strongly correlated systems, paving the way for future studies that might overcome the current limitations by generating or accessing more comprehensive datasets.

## 8 Appendices

### 8.1 Detailed Code

The comprehensive source code utilized for this study’s simulations has been made publicly available for review and reuse. For detailed examination and further reference, please visit our GitHub repository at the following URL: <https://github.com/33ron33/ML-DMFT>.



## References

- Anderson, P. W. (1961). Localized magnetic states in metals. *Physical Review*, 124(1), 41.
- Caffarel, M., & Krauth, W. (1994). Exact diagonalization approach to correlated fermions in infinite dimensions: Mott transition and superconductivity. *Physical review letters*, 72(10), 1545.
- Dagotto, E. (1994). Correlated electrons in high-temperature superconductors. *Reviews of Modern Physics*, 66(3), 763.
- Georges, A., & Kotliar, G. (1992). Hubbard model in infinite dimensions. *Physical Review B*, 45(12), 6479.
- Georges, A., Kotliar, G., Krauth, W., & Rozenberg, M. J. (1996). Dynamical mean-field theory of strongly correlated fermion systems and the limit of infinite dimensions. *Reviews of Modern Physics*, 68(1), 13.
- Georges, A., & Krauth, W. (1993). Physical properties of the half-filled hubbard model in infinite dimensions. *Physical Review B*, 48(10), 7167.
- Hubbard, J. (1964). Electron correlations in narrow energy bands iii. an improved solution. *Proceedings of the Royal Society of London. Series A. Mathematical and Physical Sciences*, 281(1386), 401–419.
- Jarrell, M. (1992). Hubbard model in infinite dimensions: A quantum monte carlo study. *Physical review letters*, 69(1), 168.
- J. Ohkawa, F. (1991). Electron correlation in the hubbard model in  $d=\infty$  dimension. *Journal of the Physical Society of Japan*, 60(10), 3218–3221.
- Kuramoto, Y., & Watanabe, T. (1987). Theory of momentum-dependent magnetic response in heavy-fermion systems. In *Proceedings of the yamada conference xviii on superconductivity in highly correlated fermion systems* (pp. 80–83).
- Laloux, L., Georges, A., & Krauth, W. (1994). Effect of a magnetic field on mott-hubbard systems. *Physical Review B*, 50(5), 3092.
- Metzner, W., & Vollhardt, D. (1989). Correlated lattice fermions in  $d=\infty$  dimensions. *Physical review letters*, 62(3), 324.
- Mott, N. F. (1961). The transition to the metallic state. *Philosophical Magazine*, 6(62), 287–309.
- Müller-Hartmann, E. (1989). Fermions on a lattice in high dimensions. *International Journal*

- of Modern Physics B*, 3(12), 2169–2187.
- Pruschke, T., Cox, D. L., & Jarrell, M. (1993). Hubbard model at infinite dimensions: Thermodynamic and transport properties. *Physical Review B*, 47(7), 3553.
- Rozenberg, M., Kotliar, G., & Zhang, X. (1994). Mott-hubbard transition in infinite dimensions. ii. *Physical Review B*, 49(15), 10181.
- Rozenberg, M., Zhang, X., & Kotliar, G. (1992). Mott-hubbard transition in infinite dimensions. *Physical review letters*, 69(8), 1236.
- Rozenberg, M. J., Moeller, G., & Kotliar, G. (1994). The metal–insulator transition in the hubbard model at zero temperature ii. *Modern Physics Letters B*, 8(08n09), 535–543.
- Schweitzer, H., & Czycholl, G. (1991). Weak-coupling treatment of the hubbard model in one, two and three dimensions. *Zeitschrift fuer Physik B. Condensed Matter;(Germany)*, 83(1).
- Wolff, P. A. (1961). Localized moments in metals. *Physical Review*, 124(4), 1030.
- Yamada, K. (1975). Perturbation expansion for the anderson hamiltonian. ii. *Progress of Theoretical Physics*, 53(4), 970–986.
- Yosida, K., & Yamada, K. (1970). Perturbation expansion for the anderson hamiltonian. *Progress of Theoretical Physics Supplement*, 46, 244–255.
- Yosida, K., & Yamada, K. (1975). Perturbation expansion for the anderson hamiltonian. iii. *Progress of theoretical physics*, 53(5), 1286–1301.
- Zaanen, J., & Sawatzky, G. (1987). The electronic structure and superexchange interactions in transition-metal compounds. *Canadian journal of physics*, 65(10), 1262–1271.
- Zlatić, V., Horvatić, B., & Šokćević, D. (1985). Density of states for intermediate valence and kondo systems. *Zeitschrift für Physik B Condensed Matter*, 59, 151–157.